Practical Identifiability Analysis of a Minimal Cardiovascular System Model

Antoine Pironet[*,1], Paul D. Docherty[2], Pierre C. Dauby[1], J. Geoffrey Chase[2], Thomas Desaive[1]

[*]Corresponding author

[1]GIGA-Cardiovascular Sciences
University of Liège
B5a, Quartier Agora
Allée du 6 août, 19
4000 Liège, Belgium
e-mail: a.pironet@ulg.ac.be
Phone: +32 4 366 33 56

[2]Department of Mechanical Engineering
University of Canterbury,
Private Bag 4800
Christchurch 8140, New Zealand

Abstract

Background and objective

Mathematical models of the cardiovascular system involve parameters that can be used to monitor cardiovascular state, such as volume status, vessel elastance and resistance. To do so, the model parameters have to be estimated from data collected at the patients bedside. This work deals with a minimal model of the cardiovascular system and investigates whether all its parameters can be uniquely determined from clinically available data.

Methods

An error vector was built, representing the error between seven clinically available haemodynamic measurements and the corresponding simulated values. The sensitivity of this error vector to each model parameter was first analysed, as well as the collinearity between parameters. Then, to assess practical identifiability of the parameters, profile-likelihood curves were constructed for each of the seven model parameters.

Abbreviations: CVS: Cardiovascular system; SBV: total stressed blood volume; SV: stroke volume; ICU: intensive care unit; LVEDV: left ventricular end-diastolic volume; LVESV: left ventricular end-systolic volume.

Results

Four of the seven model parameters representing left ventricular and aortic elastances, circulatory resistance and mitral valve resistance, were shown to be practically identifiable from the selected data. The remaining three parameters are practically non-identifiable. Among these parameters, output valve resistance, one can be decreased as much as possible. The other two parameters, venous elastance and total stressed blood volume, are inversely correlated, which prevents their precise estimation.

Conclusions

This work presented the practical identifiability analysis of a minimal cardiovascular system model from a limited amount of clinically available data. presented in this work The analysis showed that some of the parameters were practically non-identifiable, thus preventing the use of the model as a monitoring tool. caution needs to be taken when identifying model parameters with a limited amount of data. In particular, some parameters require The practically non-identifiable parameters could be made identifiable using more or better quality data to be practically identifiable.

Keywords

Practical identifiability; cardiovascular system; mathematical model; parameter identification.

1 Introduction

Mathematical models of the cardiovascular system (CVS) can be used with clinical data to monitor cardiac and circulatory state. To have clinical value, these models must be patient-specific. Hence, the model parameters have to be estimated from data such that model simulations represent the individual patient's state [20, 37, 28, 10]. *Parameter estimation methods and available data thus constrain the model design and identified parameters.*

There are two extreme approaches to CVS modeling. The first deals with complex three-dimensional finite element models, involving millions of degrees of freedom [13]. These models can be used to gain understanding on local parts of the CVS. The second modeling approach deals with lumped-parameter models [4]. These models represent large sections of the CVS as single elements, chambers or resistances, for example, and thus involve lumped parameters reflecting the global state of a patient.

Because of their lower number of unknown parameters, lumped-parameter models can be more readily identified from clinical data and in real time [29, 10]. The CVS model presented in this work is a simple lumped-parameter one, describing the whole CVS using three state equations and seven parameters (see Figure 1). This model is the simplest possible closed-loop model of the CVS. Very similar models have been used for precise modelling of ventricular contraction [5] and study of averaged CVS dynamics [21].

From an experimental point of view, the three-chamber CVS model has been used to compute total stressed blood volume and use this parameter as an index of fluid responsiveness [25, 26]. The values of other model parameters, such as circulatory resistance, ventricular end-systolic elastance and aortic elastance, are also useful to clinicians, to assess the cardiac and circulatory state. Furthermore, a nearly identical model has been used to estimate cardiac output in animals equipped with a left ventricular assist device [33]. Finally, many other models, more complex, can be seen as extensions of this simplest model [27, 36, 40, 37, 34, 20, 10].

Optimising the parameters of a model typically requires many model simulations. Because of the time required to perform a single simulation of a finite-element CVS model, these models cannot currently be used to perform real-time cardiac and circulatory monitoring. Lumped-parameter models, on the other hand, can be simulated much faster, which means that parameter identification can often be performed in real time [29].

1.1 Identifiability analyses

For CVS models to be used as diagnostic tools, their parameters need to be uniquely identifiable. Determining if a model is identifiable involves investigating if all parameters of this model can be uniquely determined from the measured set of model outputs. There exist three different types of identifiability analyses, according to whether the data is considered noise-free and/or continuously sampled.

Structural (also called *a priori* or theoretical) identifiability analysis considers the available data to be noise-free and continuously sampled. Hence, there is an assumption that the output data is continuous, noise-free, and infinitely differentiable [41]. Such an analysis thus focuses on the model equations and structure, and investigates if the relations between the measured outputs and the parameters allow unique retrieval of the parameters. Structural identifiability can be assessed using several methods, including differential algebra [1, 14, 16], state isomorphism [41], and power series expansion [16, 31, 41].

A posteriori (also called sensitivity-based [16]) identifiability analysis considers the data to be noise-free, but sampled at a finite number of time points. The goal of an *a posteriori* analysis is to investigate whether the quantity of experimentally available data is sufficient to uniquely determine all parameters. The quality of the data is thus irrelevant, and this analysis does not require experimental data. Methods to test *a posteriori* identifiability include parameter sensitivity analysis [16, 3] and parameter correlation analysis [16, 3].

In contrast, a practical identifiability analysis takes into account the imperfect nature of the data, for instance the sampling of the data, and the measurement and modeling errors [7]. Structural identifiability is a necessary condition for practical identifiability.

Practical identifiability analysis takes into account the quality of the data, namely their sampling and the measurement and modeling errors [16, 7]. The question is thus whether the parameters still can be uniquely determined under real experimental conditions. A practical identifiability analysis requires actual experimental data. Methods to test for practical identifiability include Monte Carlo simulations [16, 7] and building the parameters' profile likelihood curves [32, 2].

1.2 Goal

This work investigates the usability of the CVS model of interest in intensive care units (ICUs). However, as will be explained further in detail, available ICU data is often not continuous, but rather consists in beat-to-beat indices, such as means or ranges of pressures or volumes during one cardiac cycle.

A structural identifiability analysis of a generic the CVS model of interest has previously been presented [23]. This analysis was performed using a modified version of the differential algebra approach, to take into account the beat-to-beat nature of ICU data. This analysis concluded that the seven model parameters could be identified from clinically available data, under the assumption that these data are perfect.

The logical next step is to investigate if such a result remains true when using real discrete experimentally measured data. Therefore, the goal of this study is to perform investigate the practical and *a posteriori* identifiability analyses of the lumped-parameter CVS model of interest, from beat-to-beat ICU data.

2 Methods

2.1 Cardio-vascular system model

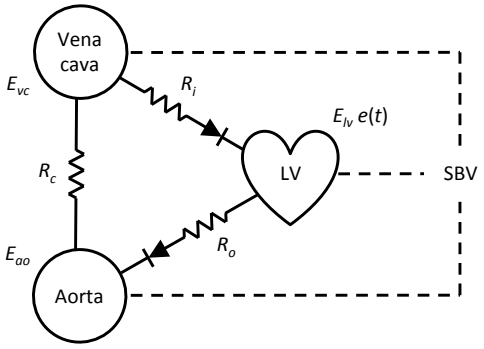

Figure 1: Schematic representation of the CVS model.

The minimal lumped-parameter CVS model used is presented in Figure 1. It consists of three elastic chambers representing the left ventricle (lv), the aorta (ao) and one vena cava (vc). The aorta and the vena cava are described by:

$$P_{ao}(t) = E_{ao}\ V_{S,ao}(t) \tag{1}$$

$$P_{vc}(t) = E_{vc}\ V_{S,vc}(t), \tag{2}$$

where P is pressure, E is elastance and V_S is stressed volume. Stressed volume represents the part of total volume that contributes to pressure generation [28].

The left ventricle is represented using the description of [38]:

$$P_{lv}(t) = E_{lv}\ e(t)\ V_{S,lv}(t), \tag{3}$$

where E_{lv} is the maximum or end-systolic elastance, and $e(t)$ is a time-varying parameter called the driver function. The driver function represents the time-varying normalised elastance of the left ventricle. It can take different forms, but for the model to correctly mimic the left ventricular behaviour, the driver function must be T-periodic, T being the cardiac period, and range from nearly 0 (during diastole, when the heart is relaxed) to 1 (at end-systole, when the heart is at its maximum stiffness). Several analytical models for the driver function have been proposed in the literature [28, 4, 5].

The three chambers are linked by vessel resistances R_c, R_o and R_i, respectively representing the circulation, the output valve and the input valve. Flow Q_c through the circulation is described by:

$$Q_c(t) = \frac{P_{ao}(t) - P_{vc}(t)}{R_c}. \tag{4}$$

The model assumes that: (i) there is flow through the valves only if the pressure gradient is positive; and (ii) the flow through an open valve can also be described by Equation 4, yielding:

$$Q_i(t) = \begin{cases} \frac{P_{vc}(t) - P_{lv}(t)}{R_i} & \text{if } P_{vc}(t) > P_{lv}(t) \\ 0 & \text{otherwise} \end{cases} \tag{5}$$

$$Q_o(t) = \begin{cases} \frac{P_{lv}(t) - P_{ao}(t)}{R_o} & \text{if } P_{lv}(t) > P_{ao}(t) \\ 0 & \text{otherwise.} \end{cases} \tag{6}$$

Finally, the continuity equation gives the rate at which the volume of the chambers change:

$$\dot{V}_{S,lv}(t) = Q_i(t) - Q_o(t), \tag{7}$$

$$\dot{V}_{S,ao}(t) = Q_o(t) - Q_c(t), \tag{8}$$

$$\dot{V}_{S,vc}(t) = Q_c(t) - Q_i(t). \tag{9}$$

These equations state that the change of a chamber's stressed volume, $\dot{V}_S$, is equal to the difference between flows coming into and going out of the chamber.

Summing the previous equation for all model chambers gives:

$$\dot{V}_{S,lv}(t) + \dot{V}_{S,ao}(t) + \dot{V}_{S,vc}(t) = 0. \tag{10}$$

Since the CVS model is a closed loop, the flow coming out of a chamber is the flow going into the next one, which explains why the right-hand side of the previous equation is zero.

$$\dot{V}_{S,lv}(t) + \dot{V}_{S,ao}(t) + \dot{V}_{S,vc}(t) = 0. \tag{11}$$

Consequently, the total stressed blood volume $V_{S,tot}$ contained in the system is a constant model parameter:

$$V_{S,lv}(t) + V_{S,ao}(t) + V_{S,vc}(t) = V_{S,tot}. \tag{12}$$

For large time scales, $V_{S,tot}$ is not necessarily constant. Indeed, total stressed volume can be modified by sympathetic nervous actions, time-dependent vascular properties, fluid exchange through the capillaries, haemorrhage, and others [8, 39]. Equally, clinical treatment can add fluid. However, the total stressed volume is constant over short and intermediate periods.

Overall, the model has seven parameters ($n = 7$ components, three elastances E_{lv}, E_{ao} and E_{vc}, three resistances R_i, R_o and R_c, and $V_{S,tot}$) and one time-varying parameter, the driver function $e(t)$. The parameter vector is thus defined:

$$\mathbf{p} = (E_{lv}\ E_{ao}\ E_{vc}\ R_i\ R_o\ R_c\ V_{S,tot}). \tag{13}$$

The T-periodic driver function, $e(t)$, was intentionally left out of the parameter vector. The cardiac period is indeed trivial to obtain from any haemodynamic

signal, and the particular form of the driver function does not matter in the following specific analysis, as long as it satisfies the criteria introduced in this section.

Matlab (2014b, MathWorks, Natick, MA) was used to solve model equations and perform the parameter identification procedures. It was run on a standard laptop computer.

2.1.1 Simulation

Figure 2 displays the result of a simulation of the CVS model using the parameter values given in Table 1. These values were chosen to produce physiological pressure and volume curves. The simulation displayed in Figure 2 begins during cardiac filling, so the input valve of the heart is open, while the output valve is closed. Accordingly, flow through the input valve is positive and proportional to the pressure difference between the vena cava and the left ventricle, $P_{vc} - P_{lv}$. In contrast, flow through the output valve is zero because the pressure in the aorta, P_{ao} is higher than that in the left ventricle, P_{lv}. Consequently, venous stressed volume, $V_{S,vc}$, is decreasing, while left ventricular stressed volume, $V_{S,lv}$, is increasing. Since the left ventricle is filling, left ventricular pressure, P_{lv}, gradually increases.

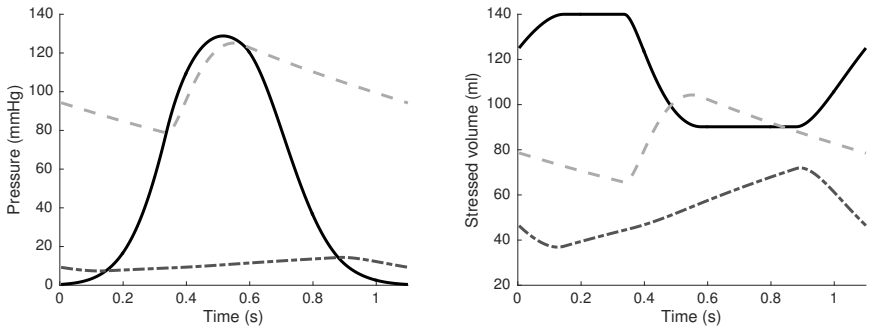

Figure 2: Simulation using the parameter values of Table 1. *Left:* venous (dash-dotted dark grey line), left ventricular (black line), and arterial (dashed light grey line) pressures. *Right:* venous (dash-dotted dark grey line), left ventricular (black line), and arterial (dashed light grey line) stressed volumes.

At a moment dictated by the driver function, $e(t)$, left ventricular contraction initiates, causing a rapid rise in left ventricular pressure, which then becomes larger than the upstream vena cava pressure. The input valve subsequently closes, marking the end of filling. This closure allows the vena cava to fill, which translates by a pressure and volume increase. Since the output valve is still closed, the left ventricular volume remains constant at its end-filling value.

Left ventricular contraction is still going on, meaning that left ventricular pressure keeps increasing, until it becomes larger than aortic pressure. At this

Table 1: Parameter values for the simulation of the CVS model presented in Figure 2. In the equation of the driver function, time, t, is expressed in seconds and "mod" denotes the modulo operator.

Parameter (units)	Value
E_{lv} (mmHg/ml)	1.4
E_{ao} (mmHg/ml)	1.2
E_{vc} (mmHg/ml)	0.2
R_i (mmHg s/ml)	0.05
R_o (mmHg s/ml)	0.04
R_c (mmHg s/ml)	2.0
$V_{S,tot}$ (ml)	250
$e(t)$ (no units)	$\exp\left[-20\left((t \bmod 1.1) - \frac{1.1}{2}\right)^2\right]$

moment, the output valve opens, marking the beginning of ejection. Blood flows to the aorta, filling the aorta and emptying the heart. Aortic pressure subsequently increases, proportionally to the increase in aortic volume.

Aortic pressure, increasing because of filling, soon passes over left ventricular pressure, which is decreasing because of the drop in left ventricular volume and because the left ventricle starts relaxing. At this moment, the output valve closes, marking the end of ejection. The output flow goes back to zero. Since the input valve is still closed, the left ventricular volume remains constant at its end-ejection value.

Finally, left ventricular pressure keeps decreasing, until it becomes lower than the upstream vena cava pressure. At this moment, the input valve opens, and the cardiac cycle resumes.

Several cardiac cycles may be simulated if desired, thanks to the periodicity of the driver function. In this work, only steady state simulations are used, and steady state is assumed to be reached after simulation of 100 cardiac cycles.

2.1.2 Output vector

The $m \times 1$ output vector that is considered in this work is:

$$\mathbf{y} = \begin{pmatrix} \max_T V_{lv}(t) - \min_T V_{lv}(t) \\ \frac{1}{T}\int_T V_{lv}(t)\ \mathrm{d}t \\ \max_T P_{vc}(t) - \min_T P_{vc}(t) \\ \frac{1}{T}\int_T P_{vc}(t)\ \mathrm{d}t \\ \max_T P_{ao}(t) - \min_T P_{ao}(t) \\ \frac{1}{T}\int_T P_{ao}(t)\ \mathrm{d}t \\ \max_T \dot{P}_{ao}(t) \end{pmatrix} = \begin{pmatrix} \mathrm{SV} \\ \bar{V}_{lv} \\ \mathrm{PP}_{vc} \\ \bar{P}_{vc} \\ \mathrm{PP}_{ao} \\ \bar{P}_{ao} \\ \mathrm{d}P_{ao}/\mathrm{d}t_{max} \end{pmatrix}. \tag{14}$$

In other words, $\mathbf{y}$ contains the following seven ($m = 7$) indices:

- Stroke volume (SV), equal to the range of left ventricular volume during one cardiac cycle,

- Mean left ventricular volume over one cardiac cycle, $\bar{V}_{lv}$
- Venous pulse pressure (PP_{vc}), equal to the range of vena cava pressure during one cardiac cycle,
- Mean vena cava pressure over one cardiac cycle, $\bar{P}_{vc}$
- Aortic pulse pressure (PP_{ao}), equal to the range of aortic pressure during one cardiac cycle,
- Mean aortic pressure over one cardiac cycle, $\bar{P}_{ao}$
- Maximum derivative of aortic pressure over one cardiac cycle, $\mathrm{d}P_{ao}/\mathrm{d}t_{max}$.

The availability of these measurements in an ICU environment is discussed in Section 4.1.

These indices are all computed on one cardiac cycle and are thus called beat-to-beat indices. In this work, they were computed at steady state, during the last of the 100 simulated cardiac cycles. As an example, the simulation presented in Figure 2 is associated to the following output vector:

$$\mathbf{y}^{model} = \begin{pmatrix} 49.82 \text{ ml} \\ 111.91 \text{ ml} \\ 7.01 \text{ mmHg} \\ 10.66 \text{ mmHg} \\ 46.41 \text{ mmHg} \\ 101.72 \text{ mmHg} \\ 370.29 \text{ mmHg/s} \end{pmatrix}. \tag{15}$$

2.2 Experimental reference data

Experimental animal data was used for parameter identification to investigate practical identifiability. This data came from measurements on one anaesthetised 27 kg pig, performed with the approval of the Ethics Commission of for the Use of Animals at the University of Liège, Belgium.

The pig was mechanically ventilated at a positive end-expiratory pressure of 5 $\mathrm{cmH_2O}$. One pig is used in this study to investigate practical identifiability from the data.

The pig was first given a muscle relaxant, sedated and anaesthetised. Mechanical ventilation was performed at a positive end-expiratory pressure of 5 $\mathrm{cmH_2O}$. After induction of anaesthesia, the animal's heart was accessed through a median sternotomy.

Catheters (Transonic, NY) were positioned to provide continuous recording of:

- Left ventricular pressure $P_{lv}(t)$,
- Left ventricular and volume $V_{lv}(t)$,

- Aortic pressure $P_{ao}(t)$,
- Inferior vena cava pressure $P_{vc}(t)$.

For the present analysis, these four measurements were studied over six consecutive respiratory cycles, recorded during steady experimental conditions. These data are displayed in Figure 3.

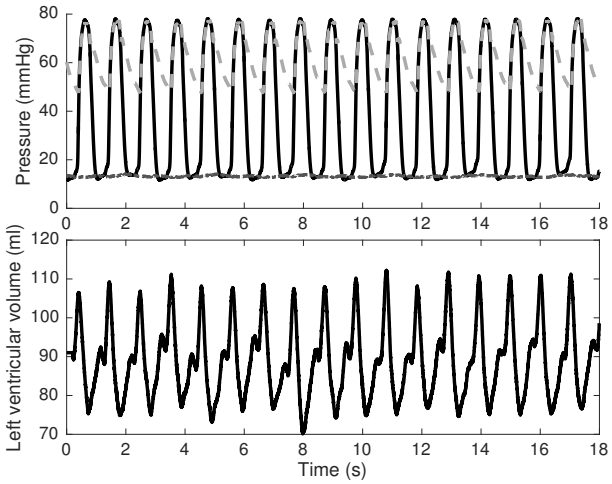

Figure 3: Experimental data. *Top:* aortic (dashed light grey line), left ventricular (black line), and venous (dash-dotted dark grey line) pressures. *Bottom:* left ventricular volume.

From these measurements, the 7 components of the output vector were calculated for each cardiac period, as dictated by Equation 14. This procedure resulted in 16 replicates of the output vector. The 16 versions of the m components of the output vector are displayed in Figure 4.

From these measurements, the following beat-to-beat indices were calculated on each cardiac period:

- Left ventricular stroke volume SV,
- Mean left ventricular volume $\bar{V}_{lv}$,
- Vena cava pulse pressure PP_{vc},
- Mean vena cava pressure $\bar{P}_{vc}$,
- Aortic pulse pressure PP_{ao},
- Mean aortic pressure $\bar{P}_{ao}$,

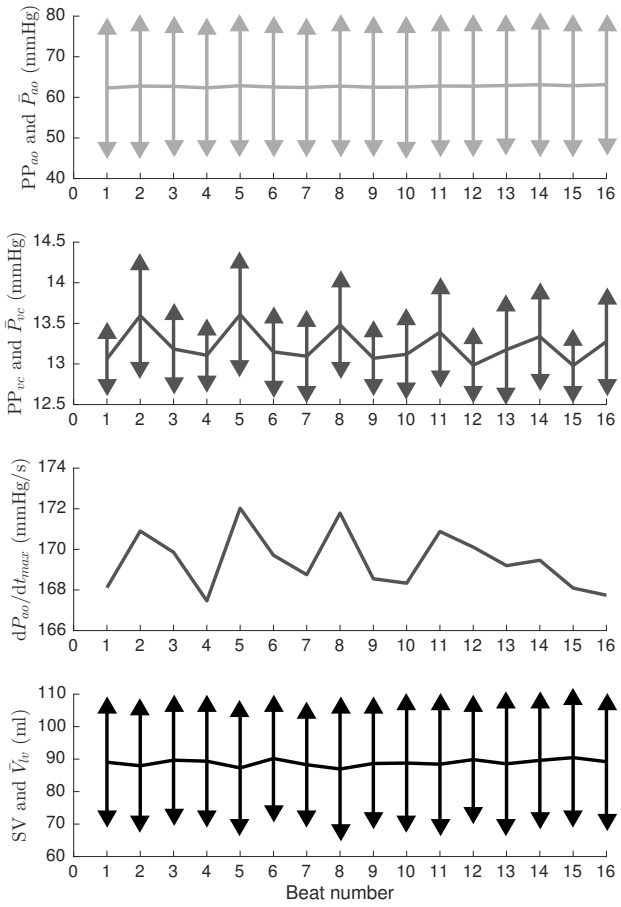

Figure 4: Components of the output vector, computed on the 16 beats of experimental data. *A:* mean aortic pressure (broken line) and aortic pulse pressure (vertical arrows). *B:* mean vena cava pressure (broken line) and vena cava pulse pressure (vertical arrows). *C:* maximum derivative of aortic pressure. *D:* mean left ventricular volume (broken line) and left ventricular stroke volume (vertical arrows).

- *Maximum derivative of aortic pressure* dP_{ao}/dt_{max}

All beat-to-beat data was averaged over six respiratory periods to neutralize The 16 replicates of the output vector were then averaged, thus neutralising

the effect of mechanical ventilation on the haemodynamic signals. This process also allowed the computation of standard errors, σ_i, for each component of the measured output vector, y_i^{data} beat-to-beat index. The mean beat-to-beat indices and their standard errors are summarised in Table 2.

Table 2: Summary of the experimental data.

i	Notation (units)	Mean, y_i^{data}	Standard error, σ_i
1	SV (ml)	34.83	1.78
2	$\bar{V}_{lv}$ (ml)	88.89	0.98
3	PP_{vc} (mmHg)	0.91	0.23
4	$\bar{P}_{vc}$ (mmHg)	13.23	0.20
5	PP_{ao} (mmHg)	29.45	0.35
6	$\bar{P}_{ao}$ (mmHg)	62.71	0.25
7	$\mathrm{d}P_{ao}/\mathrm{d}t_{max}$ (mmHg/s)	169.44	1.41

2.3 Error function

The practical identifiability analysis was carried out using the output set containing the seven beat-to-beat indices. A quadratic error function was built from this output set, and defined:

$$\psi(\mathbf{p}) = \sum_{i=1}^{7} \left(\frac{y_i^{data} - y_i^{model}(\mathbf{p})}{\sigma_i} \right)^2, \tag{16}$$

$$\begin{aligned} \psi(\mathbf{p}) \;\#\; & \left(\frac{\mathrm{SV} - \mathrm{SV}(\mathbf{p})}{\sigma_{SV}} \right)^2 + \left(\frac{\mathrm{PP}_{ao} - \mathrm{PP}_{ao}(\mathbf{p})}{\sigma_{PP_{ao}}} \right)^2 \\ & + \left(\frac{\mathrm{PP}_{vc} - \mathrm{PP}_{vc}(\mathbf{p})}{\sigma_{PP_{vc}}} \right)^2 + \left(\frac{\bar{V}_{lv} - \bar{V}_{lv}(\mathbf{p})}{\sigma_{\bar{V}_{lv}}} \right)^2 \\ & + \left(\frac{\bar{P}_{ao} - \bar{P}_{ao}(\mathbf{p})}{\sigma_{\bar{P}_{ao}}} \right)^2 + \left(\frac{\bar{P}_{vc} - \bar{P}_{vc}(\mathbf{p})}{\sigma_{\bar{P}_{vc}}} \right)^2 \\ & + \left(\frac{\mathrm{d}P_{ao}/\mathrm{d}t_{max} - \mathrm{d}P_{ao}(\mathbf{p})/\mathrm{d}t_{max}}{\sigma_{\mathrm{d}P_{ao}/\mathrm{d}t_{max}}} \right)^2, \end{aligned} \tag{17}$$

where the outputs are $y_i^{model}(\mathbf{p})$ contains the simulated outputs, depending on $\mathbf{p}$. The outputs The components y_i^{data} are the measured outputs presented in Table 2, not depending on $\mathbf{p}$. The denominator of the fraction in Equation 16 is the standard error, σ_i, related to each output measurement, also presented in Table 2. Such a formulation of the error function drives the parameter identification process towards maximum likelihood parameter values [32, 41].

2.4 *A posteriori* identifiability analysis

The aim of an *a posteriori* analysis is to know which parameters have the largest influence on the output vector. This question can be answered using the sensitivity matrix [16]. The scaled $m \times n$ sensitivity matrix, $\mathbf{S}$, contains the derivatives of the output vector, $\mathbf{y}$, with respect to the vector of model parameters, $\mathbf{p}$ [3]:

$$S_{ij} = \left.\frac{\partial y_i}{\partial p_j}\right|_{\mathbf{p}=\mathbf{p}_0} \frac{\Delta p_j}{\mathrm{SC}_i}. \tag{18}$$

In the previous equation, $\mathbf{p}_0$ denotes the initial parameter values, Δp_j is a measure of the range of p_j, and SC_i is a scaling factor for y_i. Since no information is available beforehand on the range of p_j, Δp_j can be taken as $p_{0,j}$ [3]. In the present case of weighted least squares, SC_i needs to be taken as σ_i [3]. In this work, the derivatives in the sensitivity matrix are computed by central difference approximation, which is the simplest method [3].

2.4.1 Parameter importance index

To evaluate the sensitivity, δ_j, of the output vector to the jth parameter, p_j, the following index can be computed [3]:

$$\delta_j = \sqrt{\frac{1}{m}\sum_{i=1}^{m} S_{ij}^2}. \tag{19}$$

2.4.2 Collinearity index

Computing the collinearity index allows testing if pairs of parameters exert the same influence on $\mathbf{y}$. The motivation to perform such an analysis is that, if two parameters have very similar effects on the error vector, they will not be easily identifiable together.

For the computation of the collinearity index, the normalised sensitivity matrix, $\tilde{\mathbf{S}}$, is defined as:

$$\tilde{S}_{ij} = \frac{S_{ij}}{\delta_j \sqrt{m}}. \tag{20}$$

Then, the n submatrices $\tilde{\mathbf{S}}_j$ are defined as the $m \times j$ matrices containing the j first columns of $\tilde{\mathbf{S}}$, corresponding to the output sensitivities to the j first parameters. The principle of the collinearity index is to compute the smallest eigenvalue, λ_j, of each of the $j \times j$ matrices $\tilde{\mathbf{S}}_j^T \tilde{\mathbf{S}}_j$. The index is then defined as:

$$\gamma_j = \frac{1}{\sqrt{\lambda_j}}. \tag{21}$$

The larger the index, the more the parameters p_1 to p_j are linearly related. According to Brun *et al.* [3], critical values for γ_j lie between 5 and 20.

2.5 Practical identifiability analysis

The practical identifiability analysis used in this work relies on the framework described by Raue *et al.* [32]. As mentioned in the introduction, the other methods for practical identifiability analysis involve Monte Carlo simulations. The method of Raue *et al.* was preferred because of its solid, statistically justified framework for declaring parameters practically identifiable or not, while Monte Carlo methods do not provide clear thresholds for practical identifiability [16]. In addition, the method of Raue *et al.* can easily be applied to the beat-to-beat data that is available in ICUs.

The method of Raue *et al.* is described in Appendix A. Therefore, only its basics will be recalled in this section. The main element of the method is the profile likelihood functions, ψ_{PL}, that have to be constructed for each parameter p_i. These functions follow the least steep direction on the surface of the error function, ψ. If the profile likelihood function of the parameter p_i crosses a pre-defined threshold, the parameter is declared practically identifiable.

2.6 Initial parameter values

Solving the minimisation problems stated in Equations 40 and 41 requires using a minimisation algorithm, which starts from an initial point, $\mathbf{p}_0$, provided by the user. The closer this initial point is to the optimal parameter value, $\mathbf{p}^*$, the faster the minimisation process.

In addition, the *a posteriori* analyses are local procedures, because they depend on the parameter values $\mathbf{p}_0$ at which the sensitivity matrix is computed. Consequently, for these procedures to be relevant, it is important to choose initial parameter values that are as close as possible to the optimal ones.

~~Consequently~~ For these two reasons, formulae were derived for precise computation of initial parameter values. Initial parameter values were obtained using the available data in combination with the model equations presented in Section 2.1. The derivation of the following approximate formulae is given detailed in Appendix B.

1. The cardiac period was computed as the mean distance between successive minima of aortic pressure: $T = 1.04$ s.

2. The initial value of the circulatory resistance R_c was computed as:

$$R_c = T\frac{\bar{P}_{ao} - \bar{P}_{vc}}{\mathrm{SV}} = 1.5 \text{ mmHg s/ml}. \tag{22}$$

3. Aortic elastance E_{ao} was estimated by fitting the following equation to aortic pressure during diastole:

$$P_{ao}(t) \approx \exp\left(-\frac{E_{ao}(t - t_{EE})}{R_c}\right) P_{ao}(t_{EE}). \tag{23}$$

where t_{EE} denotes the end of ejection, identified as the point at which left ventricular pressure drops below aortic pressure. The computation provided $E_{ao} = 0.98$ mmHg/ml.

4. Left ventricular end-systolic elastance E_{lv} has been computed as:

$$E_{lv} \approx \max_{T} \frac{P_{lv}(t)}{V_{lv}(t)} = 1.0 \text{ mmHg/ml}. \tag{24}$$

The driver function, $e(t)$, was then obtained as:

$$e(t) \approx \frac{P_{lv}(t)}{E_{lv}\ V_{lv}(t)}. \tag{25}$$

It was specifically found using measured left ventricular pressure for P_{lv} and left ventricular volume for V_{lv}. The resulting curve was then approximated by its Fourier series up to the tenth harmonic. This Fourier approximation was used to drive the three-chamber model. Figure 5 shows the experimental driver function and its approximation.

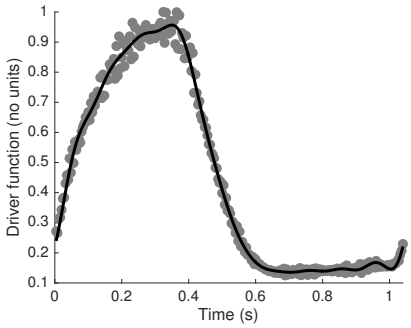

Figure 5: Experimental driver function (grey dots) and its Fourier series approximation (black line). The latter is used to drive the CVS model.

5. Output valve resistance was initialised using:

$$R_o = \frac{\int_{t_{BE}}^{t_{EE}} (P_{lv}(t) - P_{ao}(t))\ \mathrm{d}t}{\mathrm{SV}} = 0.0099 \text{ mmHg s/ml}, \tag{26}$$

where t_{BE} and t_{EE} denote the beginning and end of ejection, identified as the points at which aortic pressure crosses left ventricular pressure.

6. Input valve resistance was initialised using:

$$R_i = \frac{\int_{t_{BF}}^{t_{EF}} (P_{vc}(t) - P_{lv}(t))\ \mathrm{d}t}{\mathrm{SV}} = 0.0030 \text{ mmHg s/ml}, \tag{27}$$

where t_{BF} and t_{EF} denote the beginning and end of filling, identified as the points at which vena cava pressure crosses left ventricular pressure.

7. Venous elastance E_{vc} was estimated using:

$$E_{vc} \approx 2\frac{\mathrm{PP}_{vc}}{\mathrm{SV}} = 0.034 \text{ mmHg s/ml}. \tag{28}$$

8. To determine the initial value of $V_{S,tot}$, the following equation was used:

$$V_{S,tot} \approx \bar{V}_{lv} + \frac{\bar{P}_{ao}}{E_{ao}} + \frac{\bar{P}_{vc}}{E_{vc}} = 550 \text{ ml}. \tag{29}$$

Figure 6 displays a simulation performed using the previously computed initial parameter values.

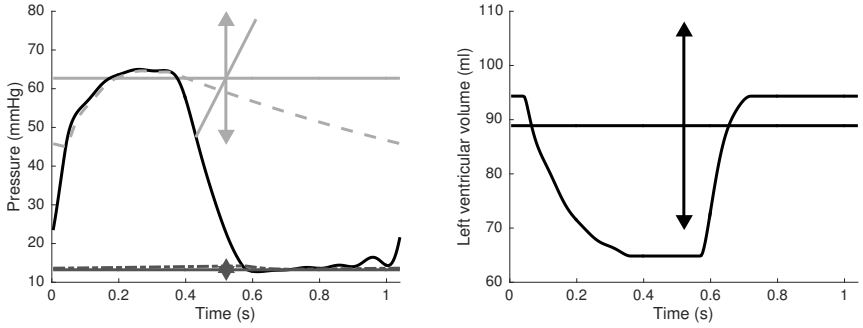

Figure 6: Model simulation using the initial parameter values. *Left:* venous (dash-dotted dark grey line), left ventricular (black line), and arterial (dashed light grey line) pressures. *Right:* left ventricular volume. For each curve except left ventricular pressure, the horizontal lines represent the reference mean, and the vertical arrows represent the reference range. The slope of the oblique, light grey line is the reference value for $\mathrm{d}P_{ao}/\mathrm{d}t_{max}$.

3 Results

3.1 Parameter importance index and collinearity index

The sensitivities, δ_j, computed using Equation 19 are displayed in Figure 7. The parameter to which the output vector, $\mathbf{y}$, is the most sensitive is $V_{S,tot}$. The 2nd to 4th most influential parameters are vena cava elastance, E_{vc}, aortic elastance, E_{ao}, and circulatory resistance, R_c. The remaining parameters are, in order of decreasing sensitivity, left ventricular elastance, E_{lv}, output valve resistance, R_o, and input valve resistance, R_i.

The computed collinearity index, γ_j, is displayed in Figure 8. As can be observed, the first six parameters are not strongly collinear with each other. However, when considering all seven parameters, the collinearity index equals 34,

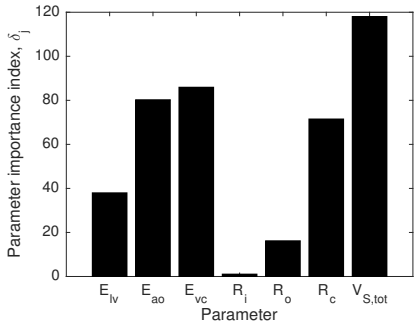

Figure 7: Parameter importance indices, δ_j, calculated from Equation 19.

indicating a strong relationship between the 7th parameter, $V_{S,tot}$, and another one. Analysing the sensitivity matrix reveals that this other parameter is E_{vc}.

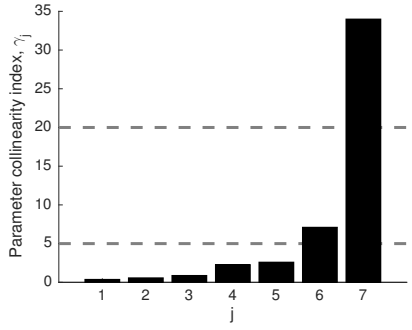

Figure 8: Parameter collinearity index, γ_j. The dashed lines indicate the maximum and minimum critical thresholds reported by Brun *et al.* [3].

3.2 Optimal parameter values

The optimal parameter values found by solving the parameter identification problem in Equation 40 are displayed in Table 3, along with their initial values. The simulation carried out using the optimal parameter values is displayed in Figure 9 and the corresponding calculated values of the beat-to-beat indices are displayed in Table 3. The corresponding value of the error is $\psi(\mathbf{p}^*) = 102.99$.

As can be seen by comparing observing Table 3, the final errors between measured and simulated mean arterial pressure, range of arterial pressure, maximum derivative of aortic pressure, mean venous pressure and mean ventricular volume are small (between 1 and 13 % below 8 %). Conversely, the simulated

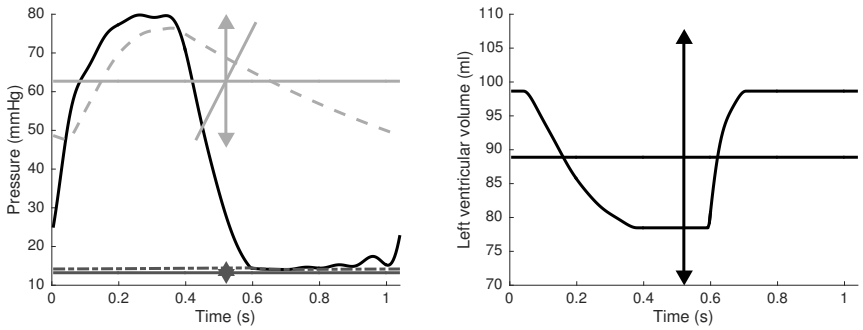

Figure 9: Model simulation using the optimal parameter values of Table 3. *Left:* venous (dash-dotted dark grey line), left ventricular (black line), and arterial (dashed light grey line) pressures. *Right:* left ventricular volume. For each curve except left ventricular pressure, the horizontal lines represent the reference mean, and the vertical arrows represent the reference range. The slope of the oblique, light grey line is the reference value for $\mathrm{d}P_{ao}/\mathrm{d}t_{max}$.

Table 3: Optimal and initial parameter values, along with corresponding simulated outputs and their references.

Parameter (units)	Initial, $\mathbf{p}_0$	Optimal, $\mathbf{p}^*$	
E_{lv} (mmHg/ml)	1.0	1.1	
E_{ao} (mmHg/ml)	0.98	2.2	
E_{vc} (mmHg/ml)	0.034	0.023	
R_i (mmHg s/ml)	0.0030	0.00010	
R_o (mmHg s/ml)	0.0099	0.11	
R_c (mmHg s/ml)	1.5	2.5	
$V_{S,tot}$ (ml)	550	760	
Output, $\mathbf{y}$ (units)	Initial	Optimal	Reference
SV (ml)	29.50	20.18	34.83 ± 1.78
$\bar{V}_{lv}$ (ml)	80.67	89.90	88.89 ± 0.98
PP_{vc} (mmHg)	0.85	0.40	0.91 ± 0.23
$\bar{P}_{vc}$ (mmHg)	13.75	14.25	13.23 ± 0.20
PP_{ao} (mmHg)	19.57	28.89	29.45 ± 0.35
$\bar{P}_{ao}$ (mmHg)	55.76	62.45	62.71 ± 0.25
$\mathrm{d}P_{ao}/\mathrm{d}t_{max}$ (mmHg/s)	256.86	169.94	169.44 ± 1.41
Objective, ψ (no units)	5482.7	102.99	

SV and range of venous pressure are respectively 42 and 56 % off the measured value.

3.3 Profile likelihood functions

Figure 10 presents the profile likelihood function for each of the seven model parameters. From this figure, the bounds of the confidence intervals on each parameters can be obtained. More specifically, as dictated by Equation 42, the two bounds are the parameter values for which the profile likelihood functions cross the threshold

$$\psi = \psi(\mathbf{p}^*) + \Delta_\alpha = 102.99 + 14.07 = 117.06. \tag{30}$$

Using this definition, the following approximate parameter confidence intervals can be obtained, as displayed in Table 4.

$$E_{lv} \in [0.90, 0.99] \text{ mmHg/ml} \tag{31}$$

$$E_{ao} \in [2.2, 3.9] \text{ mmHg/ml} \tag{32}$$

$$E_{vc} \in]0, 0.082] \text{ mmHg/ml} \tag{33}$$

$$R_i \in [0.048, 0.074] \text{ mmHg s/ml} \tag{34}$$

$$R_o \in]0, 0.034] \text{ mmHg s/ml} \tag{35}$$

$$R_c \in [2.6, 4.6] \text{ mmHg s/ml} \tag{36}$$

$$V_{s,tot} \in [300, +\infty[\text{ ml}. \tag{37}$$

The confidence intervals of the parameters E_{lv}, E_{ao}, R_o and R_c are bounded finite. This outcome proves the practical identifiability of these parameters.

Table 4: Upper and lower bounds of the likelihood-based parameter confidence intervals. To update

Parameter (units)	Lower bound	Upper bound
E_{lv} (mmHg/ml)	1.0	1.1
E_{ao} (mmHg/ml)	1.8	2.7
E_{vc} (mmHg/ml)	None	0.070
R_i (mmHg s/ml)	None	0.054
R_o (mmHg s/ml)	0.09	0.13
R_c (mmHg s/ml)	2.0	3.1
$V_{S,tot}$ (ml)	310	None

The profile likelihood for the parameter E_{vc} has a clear minimum, but flattens for small values of this parameter. Consequently, no lower bound for the confidence interval of this parameter can be found using the previously described approach. This observation implies that the parameter E_{vc} is practically non-identifiable.

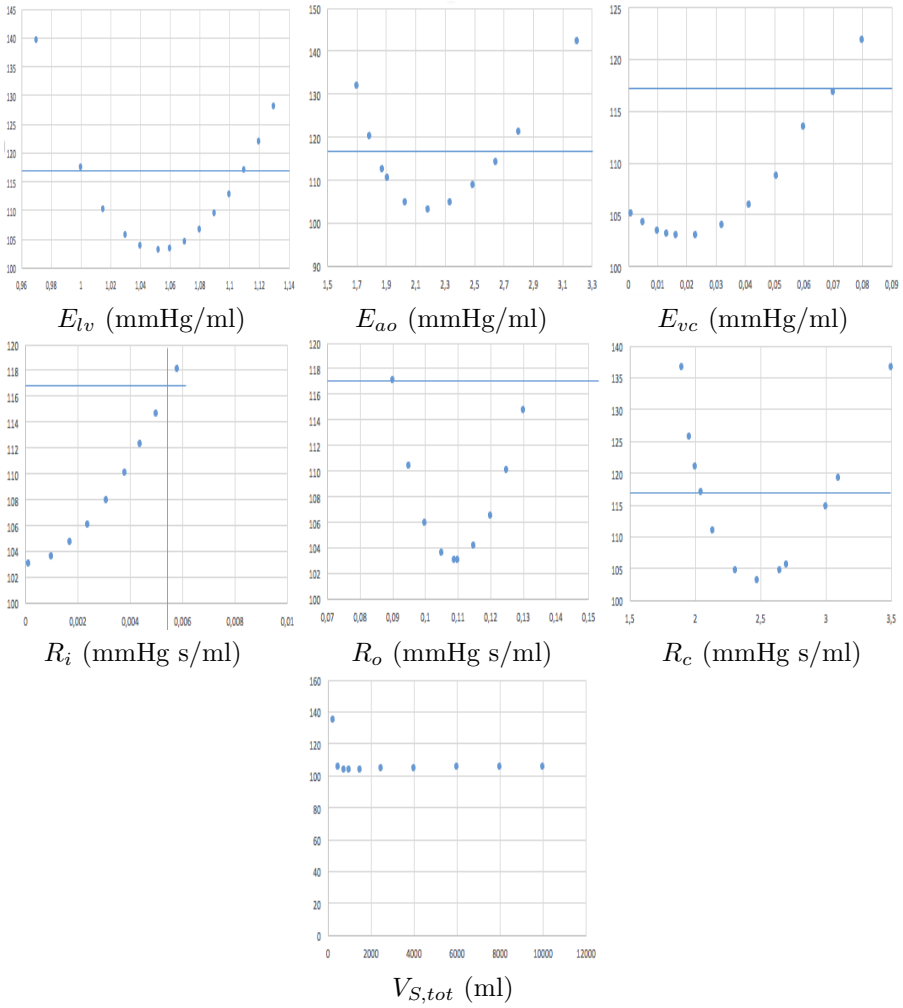

Figure 10: Profile likelihood functions for each of the seven model parameters. The star denotes the minimum value of the objective function. The horizontal dashed line denotes the threshold for practical identifiability and the vertical ones delimit the parameter confidence intervals. To update

The profile likelihood for the parameter R_i is always decreasing when this parameter decreases. Here also, no lower bound for the confidence interval of this parameter can be computed. Therefore, the parameter R_i is practically non-identifiable. The zero lower bounds given in Equations 33 and 35 come from physiological constraints.

The profile likelihood for the parameter $V_{S,tot}$ remains stationary for high values of this parameter. Consequently, the confidence interval of this parameter

has no upper bound. This observation indicates the practical non-identifiability of this parameter.

4 Discussion

4.1 Choice of the output vector

The output vector, $\mathbf{y}$, that was used in this work does not depend on time. The reason for this choice is twofold. First, the temporal evolution of all signals is not always available in the ICU, such as for ventricular volumes. Furthermore, even if haemodynamic monitors used in the ICU display the continuous pressure curves, these data cannot always be exported [6]. Consequently, only beat-to-beat indices, such as means and ranges of signals over one cardiac period, are usually available when using such monitors.

Second, the cardiac and vascular state is not usually assessed using continuous curves. Instead, clinicians use beat-to-beat indices, such as mean arterial pressure, arterial pulse pressure, mean venous pressure, or SV. The output vector used in this study contains seven beat-to-beat indices *that can be readily derived in a standard ICU environment. The clinical availability of the beat-to-beat indices*, whose clinical availability is described in this section.

First, SV can clinically be obtained using thermodilution or echocardiography [10]. Pironet *et al.* recently proved it to be a necessary measurement for identification of lumped-parameter CVS models [24]. This measurement thus had to be included in the *available data* output vector. The fact that the standard error, σ_1, was large for this measurement can be attributed to two factors: the low precision of the catheters to measure ventricular volume, and the strong influence of mechanical ventilation on SV [22], as can be observed in Figure 4.

Mean left ventricular volume, $\bar{V}_{lv}$, was also included in the output vector used in this study. Its knowledge is intuitively needed for practical identification of left ventricular end-systolic elastance, E_{lv}. Otherwise, there is no way of knowing the location of the pressure-volume loop on the volume axis, which in turn makes E_{lv} undetermined. Consequently, $\bar{V}_{lv}$ was used in this study, as it was available from the animal experimental data.

However, $\bar{V}_{lv}$ is not directly available in an ICU setting. An approximation from available ICU data is thus necessary, and can be obtained as follows. *Second,* Mean left ventricular volume can be approximated as the mean of left ventricular end-diastolic, $V_{lv}(t_{ED})$, and end-systolic, $V_{lv}(t_{ES})$, volumes:

$$\bar{V}_{lv} \approx 0.5\ V_{lv}(t_{ED}) + 0.5\ V_{lv}(t_{ES}). \tag{38}$$

Since SV is defined as the difference between $V_{lv}(t_{ED})$ and $V_{lv}(t_{ES})$, the previous equation can also be written:

$$\bar{V}_{lv} \approx V_{lv}(t_{ED}) - 0.5\ \mathrm{SV}. \tag{39}$$

Pironet et al. showed that LVEDV could be derived The remaining unknown volume, $V_{lv}(t_{ED})$, can be obtained using echocardiography [10] or approximated

from the measurement of global end-diastolic volume provided by cardiovascular monitoring devices using thermodilution [30].

Third, Systemic arterial pressure, $P_{ao}(t)$, can be obtained using an arterial line. This measurement allows the computation of $\bar{P}_{ao}$, PP_{ao}, $\mathrm{d}P_{ao}/\mathrm{d}t_{max}$ (as explained by Equation 14), t_{BF}, t_{EF}, t_{BE}, t_{EE}, and T, which are all needed for parameter identification. The value of $\mathrm{d}P_{ao}/\mathrm{d}t_{max}$ was included in the output vector because it is an index of contractility [17] and has been linked to identifiability of the output valve resistance [12]. However, in this work, including this measurement did not make the output valve resistance practically identifiable.

Fourth, central venous pressure, $P_{vc}(t)$, is usually provided by a central venous line. Its mean, $\bar{P}_{vc}$, and amplitude range, PP_{vc}, can then easily be obtained.

Finally, practical determination of the driver function, $e(t)$, requires simultaneous measurements of left and right ventricular pressures and volumes at different afterload levels. These measurements are not generally made in a clinical setting. However, the driver function has been shown to be relatively similar for all human hearts [35]. This makes *a priori* generic driver functions a sensible assumption, which suppresses the requirement for precise determination of this function.

4.2 Practically identifiable parameters

The length of the confidence intervals of a practically identifiable parameter can be divided by the optimal value of this parameter. The result provides a dimensionless measure of the sensitivity of the error function to this parameter. Sorting the four practically identifiable parameters in order from longest to shortest confidence interval gives: R_c, E_{ao}, R_i and E_{lv}. This ranking indicates that the error function is more sensitive to changes in E_{lv} than in R_c.

This study showed that parameters E_{lv}, E_{ao}, R_c and R_o from the three-chamber CVS model are practically identifiable. They can thus be used to assess a patient's cardio-vascular status.

The left ventricular end-systolic elastance, E_{lv}, is an index of left ventricular contractility. However, because of the model assumption that left ventricular unstressed volume is zero, in other words, $V_{S,lv} = V_{lv}$, this index is different from the widely used end-systolic elastance introduced by Suga and Sagawa [38]. While the latter requires recording left ventricular pressure and volume during changes in preload or afterload, the former can be computed from measurements available in the ICU, which represents an important advantage.

Parameters E_{ao} and R_c can be assimilated to the parameters of a two-element windkessel model [42]. Such a model has been used to assess arterial elastance and resistance for more than 100 years [42].

Finally, the parameter R_o represents the flow resistance of the output valve of the left ventricle. Therefore, R_o can be used to assess the status of this valve, from data available in the ICU.

4.3 Practical non-identifiability of R_i

As shown in Figure 10, the lower the parameter R_i, the lower the value of the error function. The main reason for this observation is linked to the fact that simulated $\bar{P}_{vc}$ is too high, compared to its reference value, as can be seen in Table 3. Furthermore, simulated $\bar{P}_{vc}$ has been observed to increase with R_i. This error is linked to the fact that reference vena cava pressure is very close to reference left ventricular pressure during diastole, as can be seen in Figure 3. Such a situation can be physiological, as the whole right circulation is located between the two points of measurement, inferior vena cava and left ventricle. However, the right circulation is not included in the model, and a vena cava pressure close to left ventricular pressure hinders cardiac filling. Consequently, for the simulated left ventricle to fill correctly, the parameter identification process tried to decrease R_i as much as possible.

The valve parameter R_i has previously been shown to be difficult to identify with precision in another study performed on the same CVS model [25]. In another model, the output valve parameter has been observed to converge slowly [11], which can also be attributed to the practical non-identifiability of this parameter. In addition, a sensitivity analysis on a six-chamber an 11-chamber CVS model also showed the two output input valve parameter to have a weak influence on the model outputs [9], as was also the case in this work.

To avoid dividing by values close to zero in the simulations performed in this work, a numerical lower bound had to be set for the parameter R_i. This bound was chosen to be 10^{-4} mmHg s/ml. This was set at 1 % of the parameter's initial value, resulting in a lower bound of $9.9 \cdot 10^{-5}$ mmHg s/ml.

The practical non-identifiability of the parameter R_i does not hinder the clinical use of the model. Indeed, as previously mentioned, this resistance lumps together the whole right circulation, from the tricuspid to the mitral valves. Relating changes in this parameter to actual physiological changes is thus difficult.

4.4 Practical non-identifiability of E_{vc} and $V_{S,tot}$

The fact that the profile likelihood for $V_{S,tot}$ (respectively E_{vc}) remains stationary for high (respectively low) values of this parameter comes from a correlation between $V_{S,tot}$ and E_{vc}. This correlation was already mentioned in Section 3.1 and is presented in Figure 11. The imposed values of $V_{S,tot}$ are displayed horizontally, and the value of E_{vc} after solving the minimisation problem in Equation 41 is displayed vertically. The five other parameters also vary during the minimisation process.

The reason for this correlation is that $V_{S,tot}$ can be increased arbitrarily if the venous elastance is decreased accordingly so that the venous chamber stores enough blood. This case results in the same values for the model outputs, except the amplitude of the venous pressure curve, PP_{vc}. For example, Figure 12 shows seven simulations of the three-chamber CVS model using parameter values along the flat portion of the profile likelihood for $V_{S,tot}$. the parameters given in Table 5. The $V_{S,tot}$ value in the left column is twice that of the right column. The

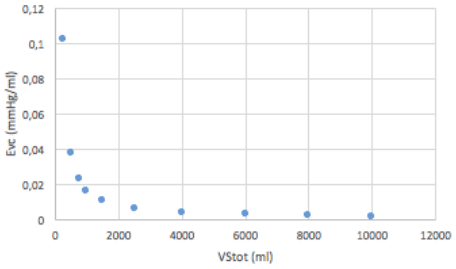

Figure 11: Correlation between the imposed values of $V_{S,tot}$ and the corresponding identified values of E_{vc} after solving the minimisation problem in Equation 41. To update.

venous elastance of the left column has been was decreased to compensate for the larger $V_{S,tot}$, thus resulting in the same mean venous pressure $\bar{P}_v$. The two simulations of Figure 12 are thus extremely similar, the only visible difference being the venous volume curve and the amplitude of the venous pressure curve, hence the lack of identifiability.

Table 5: Parameter values for the simulation of the three-chamber CVS model presented in Figure 12.

Parameter (units)	Value 1	Value 2
T (s)	1.1	1.1
E_{lv} (mmHg/ml)	1.4	1.4
E_{la} (mmHg/ml)	1.2	1.2
E_{vc} (mmHg/ml)	0.034	0.20
R_i (mmHg s/ml)	0.05	0.05
R_b (mmHg s/ml)	0.04	0.04
R_c (mmHg s/ml)	2	2
$V_{S,tot}$ (ml)	500	250
$e(t)$	$\exp\left[-20\left((t/\mathrm{mod}\,T)-\frac{T}{2}\right)^2\right]$	

Theoretically speaking, the information about the amplitude of the venous pressure curve included in the error vector should allow the method to distinguish between the two cases. However, in the data used in this work and presented in Table 2, this amplitude is very low compared to the other pressure signals, and its measurement error is high. Consequently, inconsistencies in the amplitude of the venous pressure influenced the error vector very little. As a result, using such data, the parameters are practically non-identifiable. It is expected that larger values of PP_{vc} could solve this issue. Access to the second differing output, $V_{S,vc}$, is practically impossible, because it does not correspond to an actual physical volume.

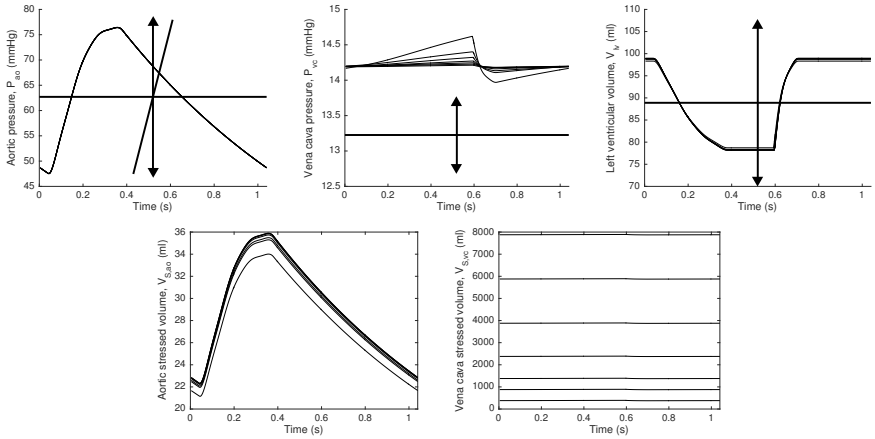

Figure 12: Superimposed time courses of the model variables for several parameter values following the profile likelihood of $V_{S,tot}$. The horizontal lines represent the reference mean, and the vertical arrows represent the reference range. The slope of the oblique line is the reference value for $\mathrm{d}P_{ao}/\mathrm{d}t_{max}$.

The practical non-identifiability of $V_{S,tot}$ could prevent the use of this parameter as an index of fluid responsiveness. Consequently, the strength of the correlation between E_{vc} and $V_{S,tot}$ should first be assessed before trying to identify the clinically important parameter $V_{S,tot}$. As previously mentioned, this correlation is expected to be lower if the amplitude of PP_{vc} is higher than in the present study. If the correlation remains strong, E_{vc} can be kept at its initial value, but the resulting identified value of $V_{S,tot}$ has to be interpreted with this assumption in mind.

Finally, the several local minima appearing on the profile likelihood functions of E_{vc} and SBV are probably also to be attributed to the correlation. Because of the correlation, the objective surface probably was very flat in the direction of the two parameters, which caused the minimisation algorithm to stop prematurely.

4.5 Comment on structural identifiability

The method developed by Raue *et al.* and used in this work allows determination of practically non-identifiable parameters as those which have infinite confidence intervals. Interestingly, this method may also evidence structurally non-identifiable parameters. Structurally non-identifiable parameters are linked by a perfect correlation so that every change in one parameter can be exactly compensated by a change in another parameter. This situation results in a uniformly flat profile likelihood curve [32].

As can be observed in Figure 10, none of the profile likelihood curves was uniformly flat, implying that no structurally non-identifiable parameters have

been detected. A previous study on the same model using an alternative analysis methodology has confirmed the absence of any structurally non-identifiable parameter from the same dataset [25]. However, the fact that no structurally non-identifiable parameters were detected does not prove structural identifiability of the model. Proving the structural identifiability of the model requires a mathematical demonstration [24].

4.6 Precision of the initial values

To evaluate the quality of Equations 22 to 29 used to compute the initial parameter values, the initial total relative error between reference and identified parameters was assessed using Table 3. Its value ranges from 5 to 2894 %, with a total error of 219 %. Interestingly, the largest error was related to the non-identifiable valve parameter, R_i. The second largest error is related to the second valve parameter, R_o, and amounts to 91 %. The high degree of error of the initial values provided by Equations 26 and 27 has previously been observed [29].

If these largest errors are not considered, the initial error on the remaining five parameters E_{lv}, E_{ao}, E_{vc}, R_c and $V_{S,tot}$ ranges from 5 to 55 %, with a total error of 66 %, indicating good precision for Equations 22, 23, 24, 28, and 29 providing suitable starting points.

4.7 Limitations

The results discussed in this study only apply to the CVS model presented in Figure 1. If a different model is investigated, the analysis should be repeated. In addition, the data used in this work comes from a single porcine experiment. Although porcine models are considered a close match for human hemodynamics, the finding of this analysis must be confirmed in a broad cohort of critically ill human patients. In particular, Docherty *et al.* found differing levels of practical identifiability depending on the patient state [7]. However, to do so, the analysis can easily be transposed to other models and data sets.

Like any other model, the minimal CVS model used in this study represents an approximation of the reality. Such simplifications are necessary to ensure identifiability of all the model parameters with readily available data. The mismatch between the model and the reality has only a small effect when using the model for monitoring cardiac and vascular state. However, predicting the effects of treatment may potentially cause larger errors because of unmodelled dynamics, such as reflex actions for example.

5 Conclusion

This work investigated the practical identifiability of the parameters of a three-chamber CVS model, from clinically available data. Elastances of the heart and aorta, as well as output mitral valve and circulatory resistance are all practically

identifiable from the data used. These parameters are important for clinicians, as they contain the essential information about the cardiac and circulatory state.

The resistance of the input mitral valve was found to be practically non-identifiable from the data used. If no supplementary data is available, this parameter has to remain constant and left out of the parameter identification process. A formula has previously been proposed to approximate the value of this parameter from clinically available data [29]. If the value of this parameter needs to be precisely known, knowing the flow through the input mitral valve, for instance using echocardiography, can solve the problem.

The total stressed blood volume parameter, $V_{S,tot}$, and the vena cava elastance, E_{vc}, were also found to be practically non-identifiable from the data used. This situation is due to a correlation between $V_{S,tot}$ and E_{vc}. This correlation is stronger if the range of vena cava pressure is small, which was the case in this work. To identify the clinically important parameter $V_{S,tot}$ with the three-chamber model, investigators should first assess the importance of the aforementioned correlation.

6 Conflict of interest statement

The authors declare that they have no conflict of interest.

7 Acknowledgement

This work was supported by the French Community of Belgium, the Belgian Funds for Scientific Research (F.R.S.-FNRS) and EU Marie Curie Actions (FP7-PEOPLE-2012-IRSES). The previous funding sources had no involvement in the design of the present study, collection, analysis or interpretation of the data, writing of the report or decision to submit it for publication.

References

[1] M. Anguelova. Nonlinear observability and identifiability: General theory and a case study of a kinetic model for S. Cerevisiae. PhD thesis, Department of Mathematics, Chalmers University of Technology and Göteborg University, 2004.

[2] S. M. Baker, C. H. Poskar, F. Schreiber, and B. H. Junker. A unified framework for estimating parameters of kinetic biological models. BMC Bioinformatics, 16:104, 2015.

[3] Roland Brun, Peter Reichert, and Hans R Künsch. Practical identifiability analysis of large environmental simulation models. Water Resources Research, 37(4):1015–1030, 2001.

[4] D. Burkhoff and J. V. Tyberg. Why does pulmonary venous pressure rise after onset of LV dysfunction: a theoretical analysis. American Journal of Physiology - Heart and Circulatory Physiology, 265(5):H1819–H1828, 1993.

[5] M. Danielsen and J. T. Ottesen. Describing the pumping heart as a pressure source. Journal of Theoretical Biology, 212(1):71–81, 2001.

[6] M. A. De Georgia, F. Kaffashi, F. J. Jacono, and K. A. Loparo. Information technology in critical care: review of monitoring and data acquisition systems for patient care and research. ScientificWorldJournal, 2015:727694, 2015.

[7] P. D. Docherty, J. G. Chase, T. Lotz, and T. Desaive. A graphical method for practical and informative identifiability analyses of physiological models: A case study of insulin kinetics and sensitivity. Biomedical Engineering OnLine, 10(1):39, 2011.

[8] J. A. Drees and C. F. Rothe. Reflex venoconstriction and capacity vessel pressure-volume relationships in dogs. Circulation Research, 34(3):360–373, 1974.

[9] L. M. Ellwein, H. T. Tran, C. Zapata, V. Novak, and M. S. Olufsen. Sensitivity analysis and model assessment: Mathematical models for arterial blood flow and blood pressure. Cardiovascular Engineering, 8(2):94–108, 2008.

[10] L. Fresiello, G. Ferrari, A. Di Molfetta, K. Zieliski, A. Tzallas, S. Jacobs, M. Darowski, M. Kozarski, B. Meyns, N. S. Katertsidis, E. C. Karvounis, M. G. Tsipouras, and M. G. Trivella. A cardiovascular simulator tailored for training and clinical uses. J Biomed Inform, 57:100–12, 2015.

[11] C. Hann, J. G. Chase, T. Desaive, C. B. Froissart, J. A. Revie, D. J. Stevenson, B. Lambermont, A. Ghuysen, P. Kolh, and G. M. Shaw. Unique parameter identification for cardiac diagnosis in critical care using minimal data sets. Computer Methods and Programs in Biomedicine, 2010.

[12] C. Hann, J. A. Revie, D. J. Stevenson, S. Heldmann, T. Desaive, C. B. Froissart, B. Lambermont, A. Ghuysen, P. Kolh, G. M. Shaw, and J. G. Chase. Patient specific identification of the cardiac driver function in a cardiovascular system model. Computer Methods and Programs in Biomedicine, 101(2):201–207, 2011.

[13] P. J. Hunter, A. J. Pullan, and B. H. Smaill. Modeling total heart function. Annual Review of Biomedical Engineering, 5(1):147–177, 2003.

[14] J. A. Kirk, M. P. Saccomani, and S. G. Shroff. A priori identifiability analysis of cardiovascular models. Cardiovasc Eng Technol, 4(4):500–512, 2013.

[15] William Q. Meeker and Luis A. Escobar. Teaching about approximate confidence regions based on maximum likelihood estimation. The American Statistician, 49(1):48–53, 1995.

[16] H. Miao, X. Xia, A. Perelson, and H. Wu. On identifiability of nonlinear ode models and applications in viral dynamics. SIAM Review, 53(1):3–39, 2011.

[17] P. Morimont, B. Lambermont, T. Desaive, N. Janssen, J. G. Chase, and V. D'Orio. Arterial dP/dt_{max} accurately reflects left ventricular contractility during shock when adequate vascular filling is achieved. BMC Cardiovascular Disorders, 12(1):13, 2012.

[18] M. C. Neale and M. B. Miller. The use of likelihood-based confidence intervals in genetic models. Behav Genet, 27(2):113–20, 1997.

[19] J. A. Nelder and R. Mead. A simplex method for function minimization. The Computer Journal, 7(4):308–313, 1965.

[20] M. S. Olufsen, J. T. Ottesen, H. T. Tran, L. M. Ellwein, L. A. Lipsitz, and V. Novak. Blood pressure and blood flow variation during postural change from sitting to standing: model development and validation. Journal of Applied Physiology, 99(4):1523–1537, 2005.

[21] T. A. Parlikar and G. C. Verghese. A simple cycle-averaged model for cardiovascular dynamics. In Engineering in Medicine and Biology Society, 2005. IEEE-EMBS 2005. 27th Annual International Conference of the IEEE, pages 5490–5494, 2005.

[22] M. R. Pinsky. Heart lung interactions during mechanical ventilation. Current Opinion in Critical Care, 18(3):256–260, 2012.

[23] A. Pironet. Model-based prediction of the response to vascular filling therapy. PhD thesis, University of Liège, Liège, Belgium, 2016.

[24] A. Pironet, P. C. Dauby, J. G. Chase, P. D. Docherty, J. A. Revie, and T. Desaive. Structural identifiability analysis of a cardiovascular system model. Med Eng Phys, 38(5):433–41, 2016.

[25] A. Pironet, P. C. Dauby, J. G. Chase, S. Kamoi, N. Janssen, P. Morimont, B. Lambermont, and T. Desaive. Model-based stressed blood volume is an index of fluid responsiveness. IFAC-PapersOnLine, 48(20):291–296, 2015. 9th IFAC Symposium on Biological and Medical Systems 2015, Berlin, Germany, 31 August-2 September 2015.

[26] A. Pironet, P. C. Dauby, P. Morimont, N. Janssen, J. G. Chase, S. Davidson, and T. Desaive. Model-based decision support algorithm to guide fluid resuscitation. IFAC-PapersOnLine, 49, 2016. 4th IFAC International Conference on Intelligent Control and Automation Sciences, Reims, France, 1-3 June 2016.

[27] A. Pironet, P. C. Dauby, S. Paeme, S. Kosta, J. G. Chase, and T. Desaive. Simulation of left atrial function using a multi-scale model of the cardiovascular system. PLoS ONE, 8(6):e65146, 2013.

[28] A. Pironet, T. Desaive, J. G. Chase, P. Morimont, and P. C. Dauby. Model-based computation of total stressed blood volume from a preload reduction manoeuvre. Mathematical Biosciences, 265:28–39, 2015.

[29] A. Pironet, T. Desaive, P. C. Dauby, J. G. Chase, and P. D. Docherty. Parameter identification methods in a model of the cardiovascular system. IFAC-PapersOnLine, 48(20):366–371, 2015. 9th IFAC Symposium on Biological and Medical Systems 2015, Berlin, Germany, 31 August-2 September 2015.

[30] A. Pironet, P. Morimont, S. Kamoi, N. Janssen, P. C. Dauby, J. G. Chase, B. Lambermont, and T. Desaive. Relation between global end-diastolic volume and left ventricular end-diastolic volume. Critical Care, 19(Suppl 1):P175, 2015.

[31] H. Pohjanpalo. System identifiability based on the power series expansion of the solution. Mathematical Biosciences, 41(12):21–33, 1978.

[32] A. Raue, C. Kreutz, T. Maiwald, J. Bachmann, M. Schilling, U. Klingmller, and J. Timmer. Structural and practical identifiability analysis of partially observed dynamical models by exploiting the profile likelihood. Bioinformatics, 25(15):1923–1929, 2009.

[33] D. Rschen, M. Rimke, J. Gesenhues, S. Leonhard, and M. Walter. Continuous cardiac output estimation under left ventricular assistance. IFAC-PapersOnLine, 48(20):569–574, 2015. 9th IFAC Symposium on Biological and Medical Systems 2015, Berlin, Germany, 31 August-2 September 2015.

[34] W. P. Santamore and D. Burkhoff. Hemodynamic consequences of ventricular interaction as assessed by model analysis. American Journal of Physiology - Heart and Circulatory Physiology, 260(Suppl 1):H146–H157, 1991.

[35] H. Senzaki, C.-H. Chen, and D. A. Kass. Single-beat estimation of end-systolic pressure-volume relation in humans: A new method with the potential for noninvasive application. Circulation, 94(10):2497–2506, 1996.

[36] B. W. Smith, J. G. Chase, R. I. Nokes, G. M. Shaw, and G. Wake. Minimal haemodynamic system model including ventricular interaction and valve dynamics. Medical Engineering & Physics, 26(2):131–139, 2004.

[37] C Starfinger, J. G. Chase, C. Hann, G. M. Shaw, P. Lambert, B. W. Smith, E. Sloth, A. Larsson, S. Andreassen, and S. Rees. Prediction of hemodynamic changes towards PEEP titrations at different volemic levels

using a minimal cardiovascular model. Computer Methods and Programs in Biomedicine, 91(2):128–134, 2008.

[38] H. Suga, K. Sagawa, and A. A. Shoukas. Load independence of the instantaneous pressure-volume ratio of the canine left ventricle and effects of epinephrine and heart rate on the ratio. Circulation Research, 32(3):314–322, 1973.

[39] M. Ursino. A mathematical model of the carotid baroregulation in pulsating conditions. IEEE Transactions on Biomedical Engineering, 46(4):382–392, April 1999.

[40] W. van Meurs. Modeling and Simulation in Biomedical Engineering: Applications in Cardiorespiratory Physiology. McGraw-Hill Professional, 2011.

[41] É. Walter and L. Pronzato. Identification of parametric models from experimental data. Communications and Control Engineering. Springer, 1997.

[42] N. Westerhof, N. Stergiopulos, and M. I. Noble. Snapshots of Hemodynamics: An Aid for Clinical Research and Graduate Education. SpringerLink : Bücher. Springer, 2010.

A Practical identifiability analysis

The practical identifiability analysis performed in this work was based on the methodology introduced by Raue *et al.* [32]. The necessary details are recalled in the following sections.

A.1 Profile likelihood

The first step of the practical identifiability analysis following the method of Raue *et al.* is the computation of the profile likelihood function, ψ_{PL}, for each parameter p_i. To compute this function, one first solves the standard parameter identification problem:

$$\mathbf{p}^* = \arg\min_{\mathbf{p}} \psi(\mathbf{p}). \tag{40}$$

That is, one needs to find the parameter vector $\mathbf{p}^*$ that minimises the error function, ψ, of Equation 16.

Then, knowing the vector $\mathbf{p}^*$, the n profile likelihood functions can be calculated for each of the n model parameters, p_i, as [32]

$$\psi_{PL}(p_i) = \min_{p_j} \psi(\mathbf{p}), \text{ with } j \in \{1, ..., n\} \backslash \{i\} \tag{41}$$

where p_i is *a priori* fixed at a value different, but close, to its optimal value p_i^*. For example, $1.1p_i^*$.

The optimisation is therefore performed on the remaining $n-1$ parameters. The procedure is then repeated for another different value of p_i, such as $1.2p_i^*$, as much as necessary to create a function of p_i. The resulting profile likelihood function helps to detect if the ψ surface is sufficiently steep across all directions to allow practical identifiability.

Matlab was used to carry out the parameter identification procedures. It was run on a standard laptop computer. Parameter identification was performed using the nonlinear simplex method of Nelder and Mead [19], starting from the previously derived initial parameter values.

A.2 Likelihood-based confidence intervals

A confidence interval for a parameter at a level of confidence $1-\alpha$ is a set that contains the true value of the parameter with a probability greater than $1-\alpha$ [18, 32]. Raue *et al.* present two approaches for computing confidence intervals: asymptotic and likelihood-based [32]. These authors recommend the use of likelihood-based confidence intervals when the amount of experimental data is low.

The likelihood-based $1-\alpha$ confidence interval of the parameter p_i is the interval [32]:

$$\{p_i \mid \psi_{PL}(p_i) - \psi(\mathbf{p}^*) < \Delta_\alpha\} \tag{42}$$

where Δ_α is a threshold depending on the desired confidence level α. In other words, the confidence interval on p_i is the set of p_i values for which the profile likelihood is lower than the optimum value of the error function, plus a given threshold. The likelihood-based 1 − α confidence interval of a parameter p_i contains the true value of the parameter with a probability greater than $1-\alpha$ [18].

The threshold Δ_α can be determined using the fact that $\psi_{PL}(p_i) - \psi(\mathbf{p}^*)$ follows a χ^2 distribution [15]. Consequently, to determine if $\psi_{PL}(p_i)$ is significantly different from $\psi(\mathbf{p}^*)$ at a level of confidence α, Δ_α must be taken as the $100(1-\alpha)$th percentile of the χ^2 distribution. Pointwise confidence intervals can be determined by using a χ^2 distribution with 1 degree of freedom. Simultaneous confidence intervals can be determined by using a χ^2 distribution with n degrees of freedom [32], where n is the number of parameters in the model in this analysis.

In the present problem, $n = 7$ and α is chosen to be 5 %. Consequently, for pointwise confidence intervals, Δ_α is equal to the 95th percentile of the χ^2 distribution with 1 degree of freedom, or 3.84 [18]. For simultaneous confidence intervals, Δ_α is the 95th percentile of the χ^2 distribution with 7 degrees of freedom, or 14.07. For increased robustness, and to account for potential underestimation of the measurement errors, simultaneous confidence intervals are used in this work.

A.3 Detection of identifiability from the profile likelihood

Using the previously described approach, three situations can be detected: structurally non-identifiable parameters, practically non-identifiable parameters and practically identifiable parameters [32]. First, if the profile likelihood of a parameter is uniformly flat, this parameter can be stated as structurally non-identifiable. Indeed, an uniformly flat profile likelihood for one parameter means that, whatever the value of the parameter, an optimal error value, $\psi(\mathbf{p}^*)$, can be retrieved by varying the other parameters. There consequently exists a functional relation between some of the parameters [32], causing their structural non-identifiability.

The profile likelihood of a structurally identifiable parameter p_i is not flat and has a clear minimum at p_i^*. For a parameter to be practically identifiable, its profile likelihood function must be steep enough, so that it crosses the Δ_α threshold for values of the parameter higher and lower than is optimal value. According to Equation 42, this situation results in a finite confidence interval for the parameter. If the profile likelihood function of a parameter is not steep enough to cross the Δ_α threshold for values of the parameter higher and lower than its optimal value, this parameter can be said to be practically non-identifiable. Consequently, a structurally non-identifiable parameter is also practically non-identifiable.

B Derivation of the initial parameter values

B.1 Input valve resistance, R_i

The combination of Equations 5 and 7 during filling ($Q_o = 0$) gives:

$$\dot{V}_{S,lv}(t) = \frac{P_{vc}(t) - P_{lv}(t)}{R_i}. \tag{43}$$

Integrating this equation from beginning (t_{BF}) to end (t_{EF}) of filling gives:

$$V_{S,lv}(t_{EF}) - V_{S,lv}(t_{BF}) = \frac{\int_{t_{BF}}^{t_{EF}} (P_{vc}(t) - P_{lv}(t))\ \mathrm{d}t}{R_i}. \tag{44}$$

Since $V_{S,lv}(t_{EF})$ is the maximum of $V_{S,lv}$ during a cardiac cycle, and $V_{S,lv}(t_{BF})$, its minimum, the left-hand side of the previous equation equals SV. Therefore, one obtains Equation 27. This equation can be graphically interpreted by stating that the area between venous and cardiac pressures during filling is equal to the product of SV and R_i.

B.2 Output valve resistance, R_o

The combination of Equations 6 and 7 during ejection, when $Q_i = 0$, reads:

$$\dot{V}_{S,lv}(t) = -\frac{P_{lv}(t) - P_{ao}(t)}{R_o}. \tag{45}$$

Integrating this equation during ejection, from t_{BE} to t_{EE}, gives:

$$V_{S,lv}(t_{EE}) - V_{S,lv}(t_{BE}) = -\frac{\int_{t_{BE}}^{t_{EE}} (P_{lv}(t) - P_{ao}(t))\ \mathrm{d}t}{R_o}. \tag{46}$$

Because $V_{S,lv}(t_{BE})$ is the maximum value of $V_{S,lv}$ and $V_{S,lv}(t_{EE})$, its minimum, the left-hand side is equal to $-\mathrm{SV}$. Rearranging terms yields Equation 26. The graphical interpretation of Equation 26 implies that the area between left ventricular and aortic pressures during ejection is equal to SV times R_o.

B.3 Circulatory resistance, R_c

The circulatory resistance can be exactly obtained using Equation 4, integrated over one cardiac cycle:

$$R_c = \frac{\int_0^T (P_{ao}(t) - P_{vc}(t))\ \mathrm{d}t}{\int_0^T Q_{vc}(t)\ \mathrm{d}t} = \frac{\bar{P}_{ao} - \bar{P}_{vc}}{\int_0^T Q_{vc}(t)\ \mathrm{d}t} T, \tag{47}$$

where $\bar{P}_{ao}$ and $\bar{P}_{vc}$ are mean aortic and vena cava pressures. The integral of the circulatory flow is equal to the blood volume going through the output valve during ejection. In turn, this volume is equal to the change of cardiac volume during ejection, SV. Therefore, Equation 22 is obtained.

B.4 Left ventricular end-systolic elastance, E_{lv}

Equation 3 can be written as:

$$\frac{P_{lv}(t)}{V_{S,lv}(t)} = E_{lv}\ e(t). \tag{48}$$

Taking the maximum of this equation over one cardiac cycle gives:

$$\max_T \frac{P_{lv}(t)}{V_{S,lv}(t)} = \max_T (E_{lv}\ e(t)) = E_{lv} \max_T e(t) = E_{lv}. \tag{49}$$

Equations 24 and 25 are obtained assuming that that left ventricular unstressed volume is zero, meaning that $V_{S,lv} = V_{lv}$. This approximation is justified in this work, because E_{lv} need not be precisely estimated. Indeed, in the data used in this work, preload and afterload do not vary. Consequently, the points of end-systole do not move, and the exact slope of the end-systolic pressure-volume relationship is not important.

B.5 Aortic elastance, E_{ao}

During diastole, volume change in the aorta is described by the combination of Equations 4 and 8:

$$\dot{V}_{S,ao}(t) = \frac{P_{ao}(t) - P_{vc}(t)}{R_c}. \tag{50}$$

If P_{vc} is neglected with respect to P_{ao} and Equation 1 is used, one gets:

$$\dot{V}_{S,ao}(t) \approx \frac{E_{ao}\ V_{S,ao}(t)}{R_c}. \tag{51}$$

Solving this ordinary differential equation for $V_{S,ao}(t)$ yields:

$$V_{S,ao}(t) \approx \exp\left(-\frac{E_{ao}\ (t - t_{EE})}{R_c}\right) V_{S,ao}(t_{EE}), \tag{52}$$

where t_{EE} denotes the end of ejection. Multiplying both sides of Equation 52 by E_{ao} yields Equation 23.

B.6 Vena cava elastance, E_{vc}

Equation 9 during systole, when $Q_i = 0$, reads:

$$\dot{V}_{S,vc}(t) = Q_c(t). \tag{53}$$

Circulatory flow is assumed to be constant and equal to its mean value, thus:

$$\dot{V}_{S,vc}(t) \approx \frac{\mathrm{SV}}{T}. \tag{54}$$

Integrating this equation from beginning, t_{BS} to end, t_{ES}, of systole gives:

$$V_{S,vc}(t_{ES}) - V_{S,vc}(t_{BS}) \approx \frac{\mathrm{SV}}{T}(t_{ES} - t_{BS}). \tag{55}$$

Multiplying both sides by E_{vc} and using Equation 2 gives:

$$P_{vc}(t_{ES}) - P_{vc}(t_{BS}) \approx E_{vc}\frac{\mathrm{SV}}{T}(t_{ES} - t_{BS}). \tag{56}$$

Finally, assuming $P_{vc}(t_{ES}) - P_{vc}(t_{BS}) \approx \mathrm{PP}_{vc}$ and $t_{ES} - t_{BS} = T/2$, one obtains Equation 28.

B.7 Total stressed volume, $V_{S,tot}$

Equation 12 is averaged on one cardiac cycle, giving:

$$\bar{V}_{S,lv} + \bar{V}_{S,ao} + \bar{V}_{S,vc} = V_{S,tot}. \tag{57}$$

Then, Equations 1 and 2 can also be averaged, yielding Equation 29.